Inter-Laminar Fault Analysis of Magnetic Cores with Grain-Oriented Electrical Steels under Harmonic Distortion Magnetisations

Hamed Hamzehbahmani, *Senior member, IEEE*

Department of Engineering, Durham University, Durham, DH1 3LE, UK
Hamed.h.bahmani@durham.ac.uk

Abstract: Inter-laminar faults (ILFs) have major impacts on the overall performance of the electrical machines and power transformers, among which extra power loss and hence lower efficiency could be highlighted. This paper presents an in depth analysis on energy loss and energy loss components of stacks of Grain-Oriented (GO) electrical steels subjected to different kinds of ILFs, under sinusoidal and non-sinusoidal inductions. Practical methods are developed to monitor quality of the magnetic cores, based on the measured static and dynamic hysteresis loops (SHL and DHL). The experimental results showed that, ILFs have a significant impact on the dynamic performance and dynamic energy loss of the cores, while their impact on the hysteresis loss is negligible. Furthermore, they become more destructive under non-sinusoidal inductions, and hence condition monitoring of the magnetic cores is more important for these applications.

1. Introduction

Electrical steels are key materials of electrical machines and transformers. For electrical steel customers the drive to lower magnetic losses to meet the challenges of global warming related regulations and tighter specification, requires every contribution to magnetic losses to be fully understood and minimised. The optimised design of the electrical machines and transformers requires higher efficiency or lower power loss, which is a key consideration for the designers and manufacturers. Considering the large numbers of electrical machines and transformers installed around the world, higher efficiency results in significant savings in energy cost and reduction in CO_2 emissions.

Electrical steels are characterised by the relative permeability and specific power loss in W/kg or total energy loss in J/m^3 during one magnetising cycle. Mechanical, magnetic and electric properties of the electrical steels can be deteriorated by manufacturing processes, e.g. welding, cutting and punching. Mechanical processes have direct impacts on quality of the materials and normal operation of the magnetic cores, and have been an active area of research for decades. Nakata *et al.* [1] and Moses *et al.* [2] have shown that the deterioration of magnetic properties due to cutting can go up to 10 mm from the cut edge. These researches indicated that, cutting a single lamination can increase the power loss by 30 %. Takahashi *et al.* [3] studied the effects of punching on magnetic properties of Non-Oriented (NO) electrical steels. Their research indicated that, the maximum relative permeability of the core can be reduced by 30 %. Wang *et al.* [4] and Zhang *et al.* [5] showed that the maximum relative permeability of welded laminations of a toroidal core with NO material can be reduced by 38 %.

Apart from the direct impacts of the manufacturing processes on magnetic properties of the electrical steels, cutting and punching of the laminations to the desirable dimensions might create microscopic edge burrs at the cut edges or around the punched holes. Burr height is typically in the range of 2 % to 10 % of the lamination thickness [6] and could lead to low inter-laminar resistance and hence inter-laminar faults (ILFs) between the adjacent laminations. ILFs lead to circulating eddy current between the defective laminations, which results in hot spot and extra localised power loss at the defective zone [7]. A few short circuits might not create high ILF currents; however, with several faults in the core the induced ILF currents could be large and cause excessive local power loss and local heating in the defective area [8]. Whereas a large number of ILFs can lead to catastrophic breakdown, the machine can still operate with a limited number of ILFs, but with elevated power loss. Local power losses result in hot spots in the core and expedite the degradation of the insulating coating and can cause premature aging of the magnetic cores.

Data sheets from the steel manufacturers typically report the specific loss figure of the materials measured at power frequencies, 50 Hz or 60 Hz, for selected peak flux densities. The standard measuring and characterising techniques of electrical steel laminations are IEC 60404-2, 2008 [9] based on Epstein frame, and BS EN 10280:2001 + A1, 2007 [10] based on Single Strip Tester (SST). Specific power loss published in the data sheets of the material, however, do not count for the geometry of the magnetic cores, and degradation of the material due to manufacturing processes. Furthermore, it is well distinguished that low inter-laminar resistance in the clamped magnetic cores due to, for example, edge burr or damage on the surface coating has a significant impact on the local and overall power loss of the magnetic cores [11-14]. Therefore, designers of the electrical machines and transformers usually find considerable deviation between the Epstein frame results and overall power losses measured from the assembled cores.

Apart from the standard methods of power loss measurements, analytical and numerical techniques have been proposed to characterise electrical steels. The first mathematical approach of this kind to determine magnetic losses was proposed by Steinmetz [15] in 1884. Other mathematical methods based on the classical hysteresis model proposed by Preisach [16] and Jiles-Atherton [17], and loss separation principle proposed by Bertotti [18] are well recognised for physicist and engineers to characterise magnetising processes and power losses of magnetic materials. The classical methods of loss prediction were initially developed for sinusoidal inductions. These methods have been modified to extend the magnetising range, also for non-sinusoidal inductions.

Magnetic cores of the modern magnetic devices, can be subjected to non-sinusoidal and distorted inductions due to, for example, magnetic saturation in the cores, and presence of power electronic converters in variable speed drives (VSDs) and renewable energy systems. Besides all of the advantages, power electronic converters are potential sources of harmonics emission. This can result in complex magnetisation regimes for the magnetic cores, and make the power loss analysis and relevant studies more complicated. Core losses, which increase rapidly with magnetising frequency, is a dominant loss component under high-frequency and harmonic distorted magnetisation conditions [20-21]; and hence ILFs become more crucial for these applications. Despite the long history of the problem and undoubted requirement for its solution, ILFs and their impacts are still questionable for certain materials and applications, e.g. under non-sinusoidal and distorted inductions. Therefore, it is timely and beneficial to extend the skills and knowledge of magnetic loss evaluation and core quality assessment of the magnetic cores under arbitrary magnetisations for modern applications. The main aim of this paper is to evaluate energy losses of magnetic cores of Grain-Oriented (GO) material under non-sinusoidal excitations, for condition monitoring and core quality assessment purposes. The study is based on the measured static and dynamic hysteresis loops (SHL and DHL). The experimental results showed that quality assessment of magnetic cores can be effectively performed by monitoring the hysteresis loops.

2. Theoretical base

Magnetising process of the magnetic materials can be analysed by means of the hysteresis phenomenon. The area enclosed by the DHL represents the total energy loss per unit volume for one magnetising cycle. Dynamic performance of GO steels can be, with high accuracy, analysed based on the statistical energy loss separation principle proposed by Bertotti [22]. In this approach, the total energy losses W_{tot}, is separated into three components, hysteresis loss W_{hys}, classical eddy current loss W_{eddy}, and excess loss W_{exc}:

$$W_{tot} = W_h + W_{eddy} + W_{exc} \quad (1)$$

Energy loss calculation and separation can be performed based on the static and dynamic hysteresis loops of the material, and therefore, loss separation of (1) can be interpreted as magnetic field separation [22]:

$$H(t) = H_h(t) + H_{eddy}(t) + H_{exc}(t) \quad (2)$$

where $H(t)$ is the magnetic field at the surface of the lamination, $H_h(t)$ is hysteresis field, $H_{eddy}(t)$ is eddy current field, and $H_{exc}(t)$ is excess field. Phenomenological concept of energy loss separation of magnetic materials can be also described by separating the total energy loss into hysteresis and dynamic losses [18-19]. In this method, both classical eddy-current and excess fields are described as dynamic field, and hence loss separation and field separation can be expressed as:

$$W_{tot} = W_h + W_{dyn} \quad (3)$$

$$H(t) = H_h(B) + H_{dyn}(t) \quad (4)$$

where $H_h(B)$ is the hysteresis field and W_h is the area of the static, or quasi-static hysteresis loop. $H_h(B)$ can be either calculated or measured under static or quasi-static conditions. Recent work conducted by the author showed that ILFs have significant impacts on the dynamic behaviour of the magnetic cores [23]. Therefore, in this paper model (3) was used in energy loss analysis and energy loss separation of the test samples.

3. Experimental set-up and Sample Preparation

Epstein size laminations (30 mm × 305 mm) with standard grades of M105-30P CGO 3 % *SiFe* (thickness $d = 0.3\ mm$ and resistivity $\rho = 0.461\ \mu\Omega m$) were provided by Cogent Power Ltd. Stacks of four laminations were prepared to simulate ILFs of different configurations. Similar to the previous work [23], artificial faults were made by applying a thin layer of lead-free solder of 10 mm wide and ~500 µm thick on sides of the stacks. The first stack, with no inter-laminar fault, was labelled as *Pack # 1*. Characteristics of this pack were considered as a reference for other measurements. Three other stacks, with ILFs, were labelled as: *Pack # 2*, Stack of laminations with ILFs at three step-like points; *Pack # 3*, Stack of laminations with ILFs at one set point and *Pack # 4*, Stack of laminations with ILFs at three set points. Perspective view of the samples are shown in Fig. 1; and side views of pack # 2 and pack # 3 are shown in figures 2-a and 2-b, respectively.

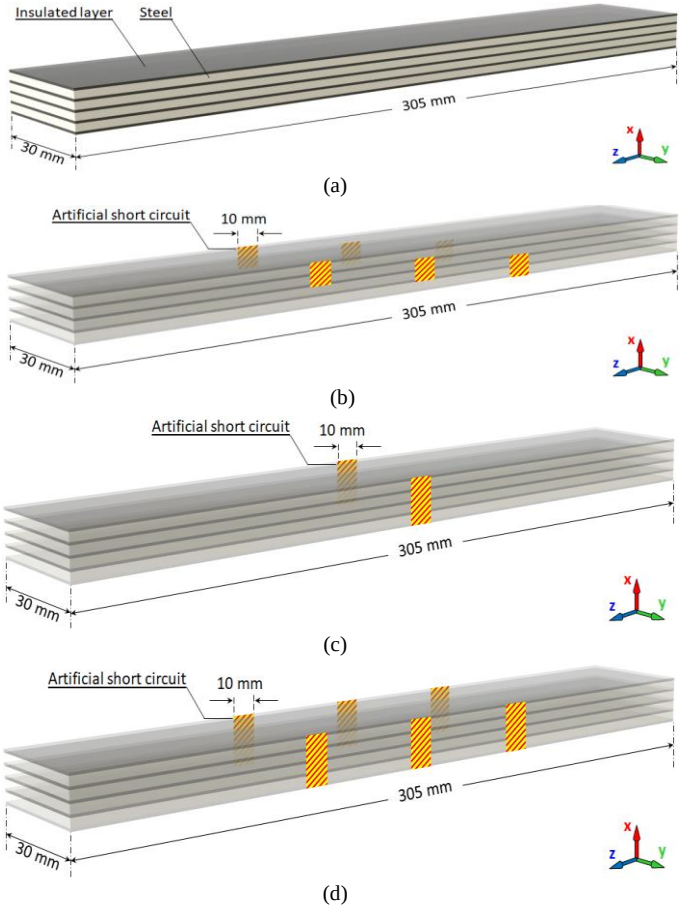

Fig. 1. *Perspective view of stacks of four laminations (a) without ILF (pack # 1); and with ILFs (b) at three step-like points (pack # 2) (c) one set point (pack # 3) and (d) at three set points (pack # 4)*

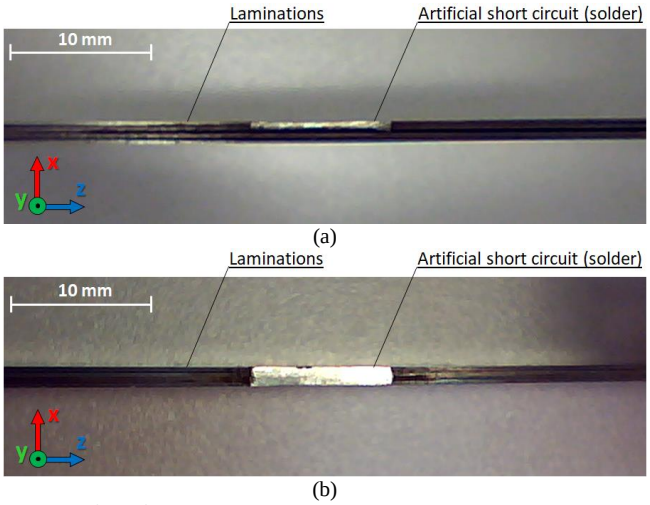

Fig. 2. *Artificial fault applied on the samples (a) pack # 2 (b) pack # 3*

In this work a standard double yoke single strip tester (SST) was used to magnetise the samples under sinusoidal induction of 50 Hz, and non-sinusoidal induction with a fundamental frequency of 50 Hz and peak flux densities of 1.1 T, 1.3 T and 1.5 T. The measuring system conforms to the British standard BS EN 10280:2007. This system shows good reproducibility of measurements for a wide range of frequency and flux density. The reproducibility of this system is characterised by a relative standard deviation of 1 % for GO materials [10]. More detail of the test setup is available in [24].

4. Experimental results

The samples were characterised by measuring the total energy losses, and monitoring the SHLs and DHLs, under sinusoidal and non-sinusoidal excitations. In the design of modern power electronic converters, it is restrictedly demanded to eliminate any even harmonic components. However odd harmonic components are generated by the power electronic converters, where the most notable components are 3rd, 5th, 7th, 9th and 11th [25]. In this paper, as an arbitrary induction waveform, non-sinusoidal induction was modelled by summation of a peak fundamental of 50 Hz, and its 3rd, 5th and 11th components at an amplitude of 10 % of the fundamental component and phase angle of 0°, as shown by (5) and Fig. 3 for a peak flux density of $B_{pk} = 1.5\ T$.

$$B(t) = B_{pk}\sin(\omega t) + 0.1\,B_{pk}\sum_{h}\sin(h\omega t) \qquad h = 3, 5, 11 \tag{5}$$

4.1. Bulk energy losses measurements:

Total energy losses of the samples under sinusoidal induction, as the most important quality indicator of the material, were initially measured at magnetising frequency of 50 Hz and peak flux densities of 1.1 T, 1.3 T and 1.5 T; the results are shown in Fig. 4. Impact of each ILF on the total energy losses under sinusoidal induction can be observed form Fig. 4. Energy loss of pack # 1, with no ILF, correlates with the nominal energy losses of the material.

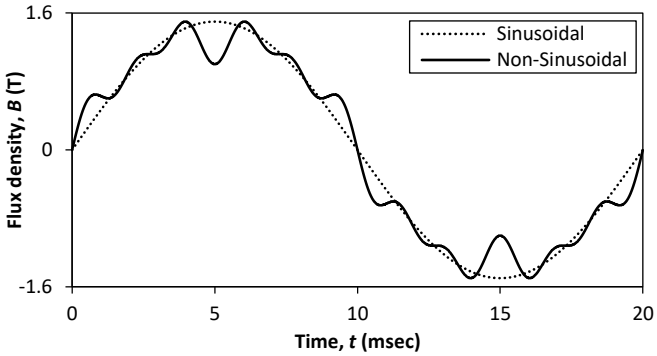

Fig. 3. *Induction waveforms at peak value of B_{pk}=1.5 T: sinusoidal induction of 50 Hz, and non-sinusoidal induction with a fundamental frequency of 50 Hz and its 3rd, 5th and 11th components*

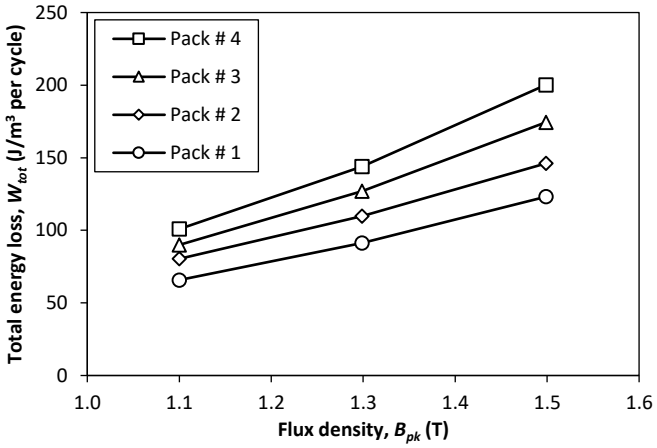

Fig. 4. *Total energy loss of the samples versus peak induction under sinusoidal magnetisation*

Although in both pack # 2 and pack # 3 all of the laminations are shorted by the artificial ILFs, total energy loss of pack # 2, with ILF at three step-like positions, is less than that of pack # 3, with ILF at one set point. Distribution of the ILF currents in the defective area and hence the extra energy losses caused by the ILFs strongly depend on size of the fault current loops, which is built upon the number of the shorted laminations. In Fig. 1-b, despite the fact that there are three fault current loops, the total energy loss is less than that of Fig. 1-c with a single fault current loop. The reason for this is related to the size of the fault current loop, which is larger in the configuration of Fig. 1-c. In this experiment the maximum energy loss was measured for pack # 4 at peak flux density of 1.5 T, which is about 63 % more than that of pack # 1. More analysis on the bulk power loss measurement of the samples under sinusoidal induction, over a wide range of frequency and flux density, is performed in [11]. The experiments were then extended to measure the total energy losses under non-sinusoidal excitation, the results are shown in Fig. 5. The same conclusions as for the case of sinusoidal excitation apply for the results of Fig. 5. However, a comparison between figures 4 and 5 shows a significant increase in the total energy losses under non-sinusoidal excitation. This experiment showed that, the maximum energy loss of pack # 4 at a peak induction of B_{pk}=1.5 T under non-sinusoidal induction is 405 J/m^3, which is about 77 % more than that of pack # 1 under the same induction.

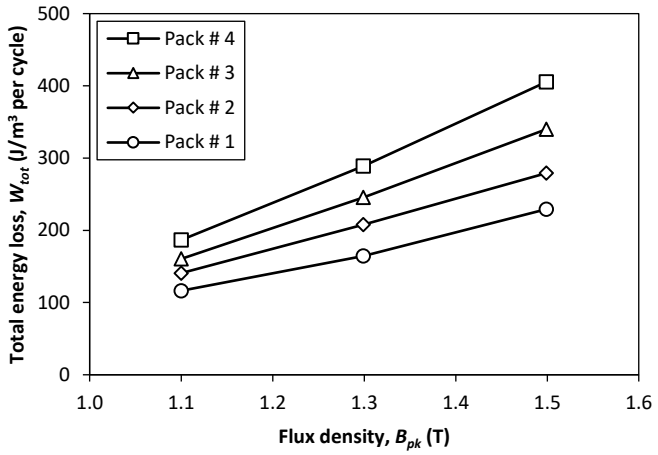

Fig. 5. *Total energy loss of the samples versus peak induction under non-sinusoidal magnetisation*

Percentage increase in the total energy loss under non-sinusoidal excitation compare to that under sinusoidal excitation is shown in Fig. 6. The total energy loss of pack # 1, with no ILF, under non-sinusoidal magnetisation at peak flux density of B_{pk}=1.5 T is about 86 % more than that under sinusoidal magnetisation. However, the percentage increase in the energy loss of pack # 2, pack # 3 and pack # 4, with ILFs, is about 91 %, 95 % and 102 %, respectively. These results clearly show that ILFs in magnetic cores become more crucial and destructive under harmonic distorted and non-sinusoidal inductions, e.g. PWM excitations.

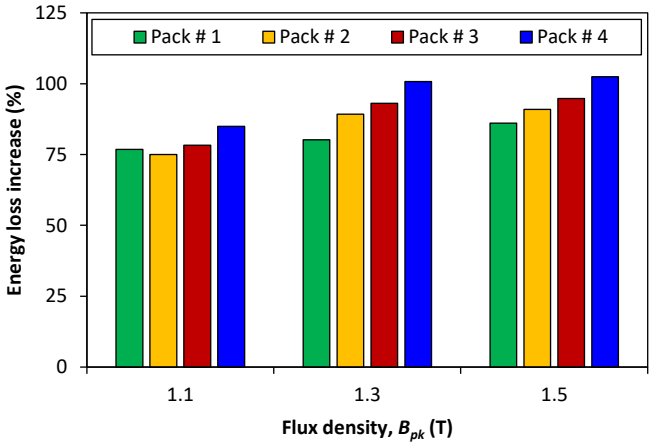

Fig. 6. *Percentage increase in total energy loss under non-sinusoidal induction*

It is well distinguished that magnetic loss, or core loss, increases rapidly with magnetising frequency, and hence it is the dominant loss component under high frequency and harmonic distorted inductions. To make a deeper insight on non-sinusoidal magnetisation of the samples, impact of each harmonic component on the total energy loss was evaluated by adding each harmonic component to the fundamental frequency. Fig. 7 shows the percentage increase in the total energy losses of the samples versus harmonic order h at a peak flux density of B_{pk}=1.5 T. Fig. 7 shows that total energy losses increase rapidly by increasing harmonic order. Furthermore, with each harmonic component, a significant increase in the energy loss was observed for pack # 2 to pack # 4. The highest increase in the energy loss was recorded for pack # 4 with 11th harmonic, which is about 70 %. With the same harmonic component, energy loss of pack # 1 was increased by about 55 %.

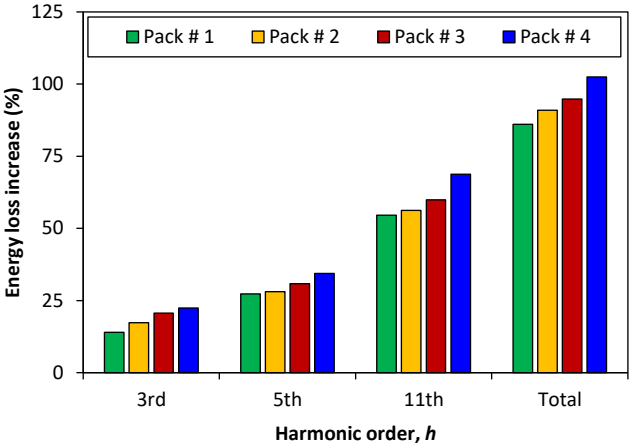

Fig. 7. *Effect of each harmonic component on the total energy loss of the samples at a peak flux density of B_{pk}=1.5 T*

4.2. Analysis on hysteresis loops

Hysteresis loops of the magnetic materials and magnetic cores may take many different shapes, which depend on the magnetising conditions, properties of the materials, and quality of the magnetic cores. Accurate measurement of the SHLs and DHLs is an adequate technique of loss evaluation over a wide range of magnetisation [23], [26-28]. Core quality assessment and energy loss evaluation of the samples were carried on by measuring and interpreting SHLs and DHLs of the samples. This can provide preliminary insight on effects of harmonic distortion on hysteresis performance of the samples. The experiments were started by measuring SHLs of the samples, which areas represent the hysteresis energy losses. The results showed that, for each flux density, SHLs of the samples fairly coincide with each other. DHLs of the samples were then measured under sinusoidal induction of 50 Hz, and peak flux densities of B_{pk}=1.1 T, B_{pk}=1.3 T and B_{pk}=1.5 T. Unlike the previous stage, a significant change in the shape and area of the DHLs was observed for different types of ILFs. A comparison between the measured DHLs under sinusoidal induction, accompanied by the measured SHL, at a peak flux density of 1.5 T is shown in Fig. 8.

The most evident feature of the DHLs of Fig. 8 is the significant increase in the hysteresis loops area and change in the loops shape, for different types of ILFs. This reflects a unique property of the DHLs in energy loss evaluation, which can be implemented in the characterisation of the magnetic cores of transformers, electrical machines and other magnetic devices with laminated cores. More analysis on the dynamic hysteresis performance of the samples under sinusoidal induction, over a wide range of frequency and flux density is available in [23]. DHLs of the samples were then measured under non-sinusoidal induction with $B(t)$ shown in Fig. 3. In order to show changes in the loop shapes due to the artificial ILFs, comparisons between the DHL of pack # 1 in pairs with those of pack # 2 to pack # 4 were performed; The results at a peak flux density of B_{pk}=1.5 T are shown in figures 9 to 11.

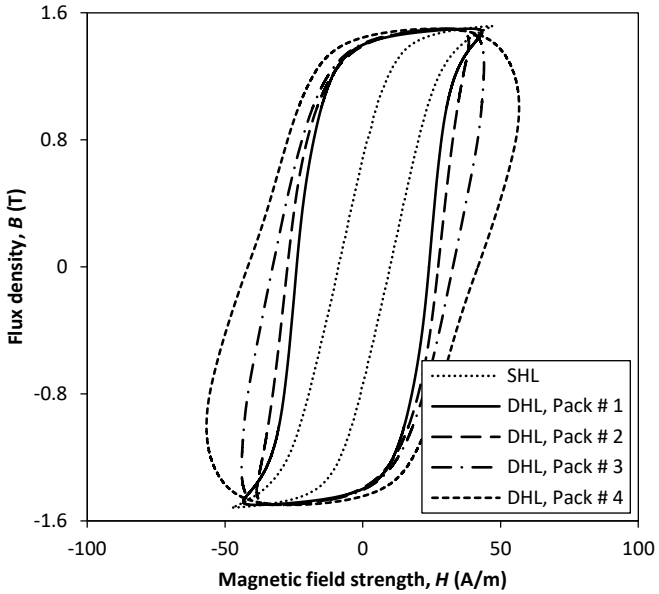

Fig. 8. *DHLs of the samples measured by SST under sinusoidal induction at a magnetising frequency of 50 Hz and a peak flux density of B_{pk}=1.5 T*

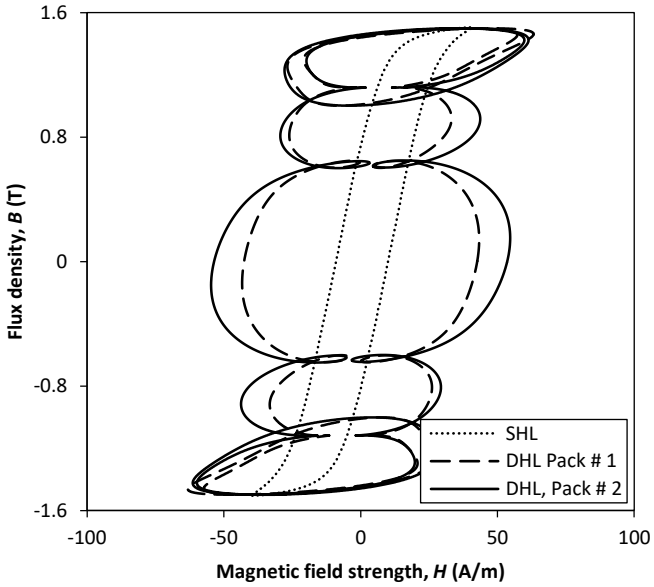

Fig. 9. *Comparison between DHL of pack # 1 and pack # 2 under non-sinusoidal magnetisation at fundamental frequency of 50 Hz and B_{pk}=1.5 T*

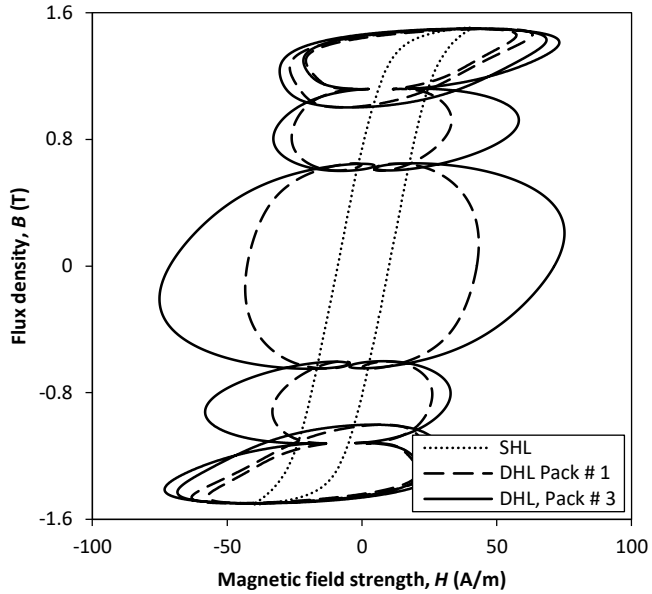

Fig. 10. *Comparison between DHL of pack # 1 and pack # 3 under non-sinusoidal magnetisation at fundamental frequency of 50 Hz and B_{pk}=1.5 T*

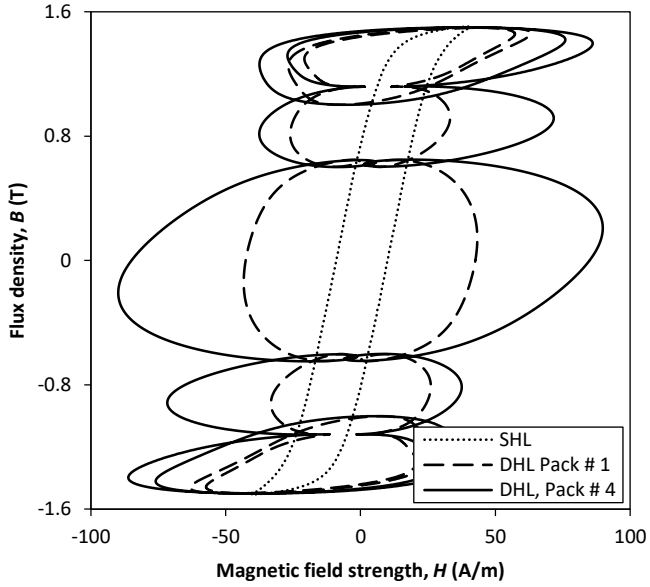

Fig. 11. *Comparison between DHL of pack # 1 and pack # 4 under non-sinusoidal magnetisation at fundamental frequency of 50 Hz and B_{pk}=1.5 T*

In these experiments a significant change in area of the DHLs of pack # 2 to pack # 4 was observed, which indicate the extra energy losses caused by the artificial faults. Recall from the preceding section, the artificial fault of pack # 3 is more destructive than that of pack # 2. Moreover, the artificial fault of pack # 4 with three fault current loops is more destructive than pack # 3. These facts can be effectively concluded by interpreting the DHLs of the samples shown in figures 9 to 11.

4.3. Analysis on energy loss components

From (3) the area between the SHLs and DHLs represents the dynamic energy loss per cycle (W_{dyn}). Figures 8 to 11 convey an important fact that the ILFs have a significant impact on the dynamic energy losses, while their impact on the hysteresis energy losses is negligible.

Dynamic energy loss of each sample under sinusoidal and non-sinusoidal inductions were calculated; the results are shown in figures 12-a and 12-b, respectively. Fig. 12-a shows a significant increase in the dynamic energy losses of pack # 2 to pack # 4 compare to the dynamic energy loss of pack # 1. The same conclusion applies when the samples are magnetised with non-sinusoidal induction, as shown in Fig. 12-b; however, in this case the dynamic energy losses of the samples with ILFs are remarkably higher than that under sinusoidal excitation. The maximum dynamic energy losses were observed for pack # 4 at peak flux density of B_{pk}=1.5 T, which are 144 J/m^3 and 349 J/m^3 for sinusoidal and non-sinusoidal magnetisations, respectively. This experiment shows the impact of ILFs on dynamic performance and dynamic energy losses of the magnetic cores under non-sinusoidal and harmonic distorted inductions.

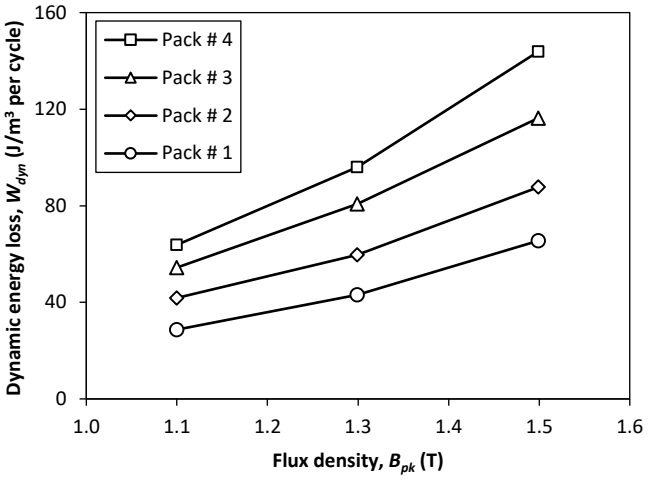

(a)

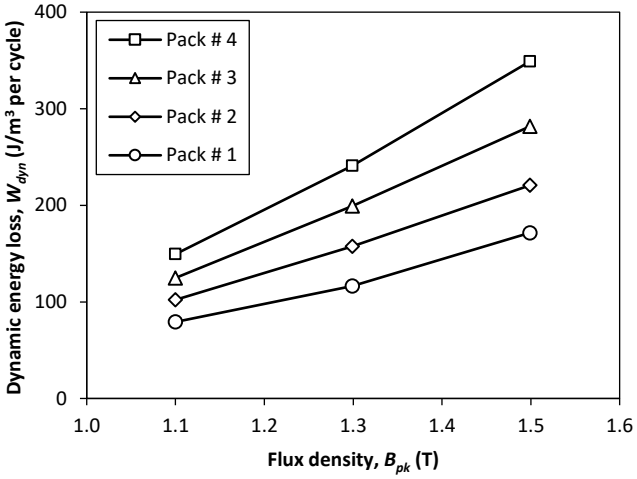

(b)

Fig. 12. *Dynamic energy loss of the samples for (a) sinusoidal magnetisation (b) harmonic distortion magnetisation*

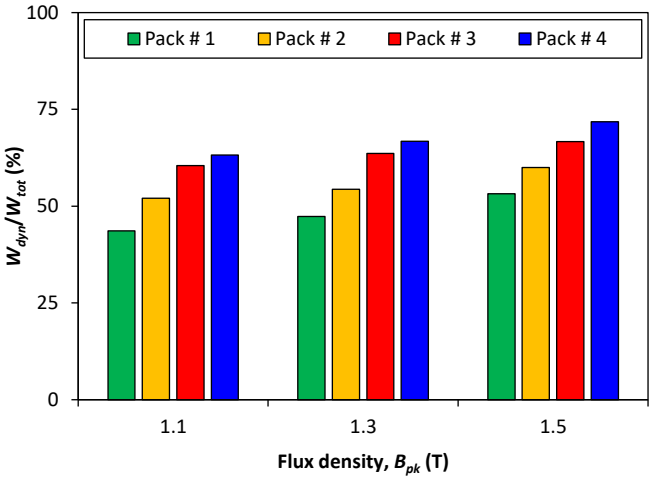

(a)

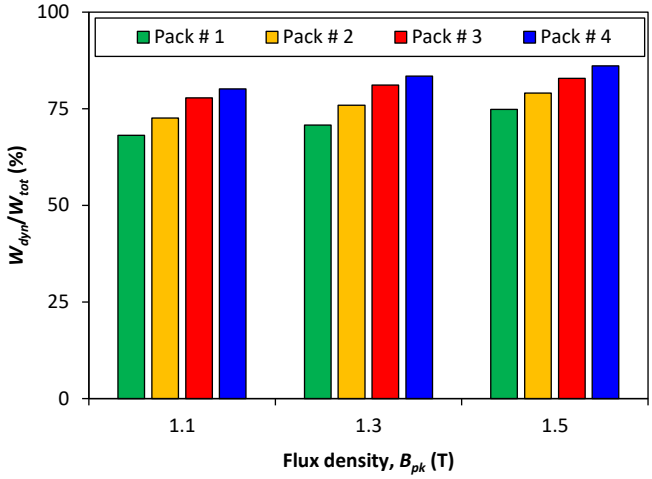

(b)

Fig. 13. *Ratio of the dynamic energy loss to the total energy loss for (a) sinusoidal magnetisation (b) harmonic distortion magnetisation*

In the last part of this study, ratio of the dynamic energy losses to the total energy losses of the samples (W_{dyn}/W_{tot}) was calculated for both sinusoidal and non-sinusoidal excitations. The results are shown in Table 1 and Fig. 13.

Table 1 Ratio of dynamic energy loss to total energy loss under sinusoidal and non-sinusoidal excitations

Excitation		W_{dyn}/W_{tot} (%)			
		Pack # 1	**Pack # 2**	**Pack # 3**	**Pack # 4**
B_{pk}=1.1 T	Sin	43.66	52.06	60.48	63.25
	Non-sin	64.14	72.61	77.84	80.13
B_{pk}=1.3 T	Sin	47.30	53.35	63.59	66.74
	Non-sin	70.73	75.88	81.14	83.43
B_{pk}=1.5 T	Sin	53.18	60.01	66.66	71.83
	Non-sin	74.84	79.09	82.89	86.09

For pack # 1, which corresponds to the nominal loss of the material, the dynamic energy loss at peak flux density of B_{pk}=1.5 T counts for 53.18 % and 74.84 % of the total energy loss for sinusoidal and non-sinusoidal excitations, respectively. However, this ratio is increased significantly for pack # 2 to pack # 4 with ILFs, as shown in Table 1. Two important notes could be concluded from this study: firstly, ILFs have a significant impact on the dynamic energy loss of the magnetic cores, while their impact on the hysteresis loss is negligible; and secondly, ILFs become more crucial under non-sinusoidal and harmonic distorted excitations. This requires special considerations on condition monitoring and quality assessment of the magnetic cores, subjected to non-sinusoidal magnetisations, e.g. power transformers and reactors used in the wind farms and other renewable energy systems.

5. Conclusion

Recent developments in the field of renewable energy systems require a major rethink on quality of the magnetic cores of the power transformers, high frequency reactors and other magnetic devices with GO steels. Power electronic converters,

as an integral part of the renewable energy systems, are potential sources of harmonic emission. Core losses, which increase rapidly with magnetising frequency, is a dominant loss component under high frequency and harmonic distorted magnetisations; and hence ILFs become more crucial for these applications. Magnetisation process of the magnetic materials under non-sinusoidal induction is a complex issue. The experimental results of this paper showed that ILFs in the magnetic cores could make the analysis even more complicated. This requires advanced techniques in condition monitoring of the magnetic cores, for energy-efficient and sustainable performance.

Due to lack of reliable models, identifying the most critical ILFs and their impacts on the performance of the magnetic cores is still a matter of intense debate across the industrial and academic communities. In this paper a new practical approach was developed for energy loss evaluation of magnetic cores with GO materials subjected to different types of ILFs, under sinusoidal and non-sinusoidal inductions. The analyses were performed based on the bulk energy loss measurements, and monitoring the SHLs and DHLs of the test samples. The experimental results showed that, ILFs become more crucial under harmonic distortion and non-sinusoidal excitations. Furthermore, ILFs have a significant impact on the dynamic energy loss of the magnetic cores, while their impact on the hysteresis loss is negligible. The experimental results also showed that ILFs can be detected with high accuracy by observing and analysing the DHLs of the magnetic cores. This is an effective technique to monitor the overall condition of the magnetic cores, and to evaluate the impact of typical ILFs on hysteresis performance and total energy loss of magnetic cores of real power transformers, high frequency reactors and other magnetic devices with GO steels.

6. Acknowledgment

The author is grateful to Cogent Power Ltd. for providing the electrical steel sheets, and Wolfson centre for magnetics at Cardiff University for the experimental work.

7. References

[1] Nakata, T., Nakano, M., and Kawahara, K. "*Effects of stress due to cutting on magnetic characteristics of silicon steel"*, IEEE Translation Journal on Magnetics in Japan, Vol. 15, Issue 2, 1991, pp 547-550

[2] Moses, A., Derebasi, N., Loisos, G. and Schoppa, A. "*Aspects of the cut-edge effect stress on the power loss and flux density distribution in electrical steel sheets"*, Journal of Magnetism and Magnetic Materials, Vol. 215-216, June 2000, pp. 690–692

[3] Takahashi, N., Morimoto, H., Yunoki, Y. and Miyagi, D. "*Effect of shrink fitting and cutting on iron loss of permanent magnet motor*", Journal of Magnetism and Magnetic Materials, Vol. 320, 2008, pp 925–928

[4] Wanga, H., Zhang, Y. and Li, S. "*Laser welding of laminated electrical steels"*, Journal of Materials Processing Technology, No. 230, 2016, pp. 99–108

[5] Zhang, Y., Wang, H., Chen, K. and Li, S. *"Comparison of laser and TIG welding of laminated electrical steels"*, Journal of Materials Processing Technology, No. 247, 2017, pp. 55-63

[6] Deng, W., Xie, Z., Lin, P. and Xu, T. "*Study on Burr Formation at the Top Edge in Rectangular Groove Cutting*", Journal of Advances in Materials Science and Engineering, Article ID 956208, Vol. 2012

[7] Bielawski, J., Duchesne, S., Roger, D., Demian, C. and Belgrand, T. "*Contribution to the Study of Losses Generated by Inter-laminar Short-Circuits*", IEEE Trans On Magn, Vol. 48, No. 4, pp 1397-1400, April 2012

[8] Lee, K., Hong, J., Lee, K., Lee, S. and Wiedenbrug, E. "*A Stator Core Quality Assessment Technique for Inverter-fed Induction Machines*", IEEE Industry Applications Society Annual Meeting, Oct 2008, pp 1-8

[9] IEC 60404-2, Magnetic materials – Part 2: Methods of measurement of the magnetic properties of electrical steel strip and sheet by means of an Epstein frame, Edition 3.1, 2008-06

[10] BS EN 10280:2001 + A1:2007, Magnetic Materials - Methods of measurement of the magnetic properties of electrical sheet and strip by means of a single sheet tester, British Standard,

[11] Hamzehbahmani, H., Anderson, P., Jenkins, K. and Lindenmo, M. "*Experimental Study on Inter-Laminar Short Circuit Faults at Random Positions in Laminated Magnetic Cores*", IET Electric Power Applications, Vol. 10, Issue 7, August 2016, pp. 604–613

[12] Bertenshaw, D., Ho, C., Smith, A., Sasi, M. and Chan, T. "*Electromagnetic modelling and detection of buried stator core faults*" IET Electric Power Applications, Vol. 11, Issue 2, March 2017, pp. 187–196

[13] Schulz, C., Duchesne, P., Roger, D. and Vincent, J. "*Capacitive Short Circuit Detection In Transformer Core Laminations*", Journal of Magnetism and Magnetic Materials 320 (2008) e911–e914

[14] Schulz, C., Roger, D., Duchesne, S. and Vincent, J., "*Experimental Characterization of Interlamination Shorts in Transformer Cores*", IEEE Trans Magn, Vol. 46, No. 2, Feb 2010, pp 614-617

[15] Steinmetz, C. "*On the law of hysteresis"*, Trans. American Institute of Electrical Engineering, No. 9, 1892, pp. 3-51

[16] Mayergoyz, I. "*Mathematical Models of Hysteresis and their Applications"*, Academic Press, 2nd Edition, 2003

[17] Jiles, D. and Atherton, D. "*Theory of ferromagnetic hysteresis"*, Journal of Magnetism and Magnetic Materials, No. 61, 1986, pp. 48–60

[18] Bertotti, G., "*General properties of power losses in soft ferromagnetic materials*", IEEE Trans. Magn., Vol. 24, No. 1, 1988, pp. 621-630

[19] Shilling, J, and Houze, G. "*Magnetic properties and domain structure in grain oriented 3% Si-Fe*" IEEE Trans. Magn., Vol. MAG-10, No. 2, Jun 1974, pp. 195–223

[20] Masisi, L., Ibrahim, M. and Wanjiku, J. "*The Effect of Two- and Three-Level Inverters on the Core Loss of a Synchronous Reluctance Machine (SynRM)*", IEEE Trans. Ind. Appl., Vol. 52, No. 2, Sep./Oct. 2016, pp. 3805-3813

[21] Zhang, Y., McLoone, S., Cao, W., Qiu, F. and Gerada, C. "*Power Loss and Thermal Analysis of a MW High Speed Permanent Magnet Synchronous Machine"*, IEEE Trans. on Energy Conversion, 32, 2017, pp. 1468-1478

[22] Bertotti, G. "*General properties of power losses in soft ferromagnetic materials*", IEEE Trans. Magn., 1988, 24, 621-630

[23] Hamzehbahmani, H. "*Development of a New Approach to Core Quality Assessment of Modern Electrical Machines*", IET Electric Power Applications, Vol 13, Issue 6, June 2019, pp. 750-756

[24] Hamzehbahmani, H., Anderson, P. and Preece, S. "*An application of an Advanced Eddy Current Power Loss Modelling to Electrical Steel in a Wide Range of Magnetising Frequency*" IET Science, Measurement & Technology, Vol. 9, Issue 7, October 2015, pp. 807-816

[25] E Fuchs and M Masoum, Power Quality in Power Systems and Electrical Machines, Academic Press, second Edition, 2015

[26] Zirka, S., Moroz, Y., Steentjes, S., Hameyer, K., Chwastek, K., Zurek, S., and Harrison, R. "*Dynamic magnetization models for soft ferromagnetic materials with coarse and fine domain structures*", Journal of Magnetism and Magnetic Materials, Vol. 394, Nov. 2015, pp 229-236

[27] Zirka, S. Moroz, Y., Moses, A. and Arturi, C. "*Static and dynamic hysteresis models for studying transformer transients*", IEEE Transaction on Power Delivery, Vol. 26, No. 4, pp. 2352-2362, Oct. 2011

[28] Alonso, C., Jazebi, S. and Leon, F. "*Experimental parameter determination and laboratory verification of the inverse hysteresis model for single-phase toroidal transformers*", IEEE Transaction on Magnetics, Vol. 52, No. 11, Nov. 2016